Performance design of high-temperature chloride salts as thermal energy storage material

Journal:	*Journal of Thermal Science*
Manuscript ID	JTS-23-0063
Manuscript Type:	Original Article
Date Submitted by the Author:	17-Feb-2023
Complete List of Authors:	Zhao, Le; North China Electric Power University, School of Energy Power and Mechanical Engineering Wang, Jingyao; North China Electric Power University, School of Energy Power and Mechanical Engineering Cui, Liu; North China Electric Power University, School of Energy Power and Mechanical Engineering Li, Baorang; North China Electric Power University, School of Energy Power and Mechanical Engineering Du, Xiaoze; North China Electric Power University, School of Energy Power and Mechanical Engineering; Lanzhou University of Technology Wu, Hongwei; University of Hertfordshire, School of Engineering and Computer Science
Keywords:	Chloride salts, thermal energy storages, thermal properties, thermal stability
Speciality:	Energy storage < Advanced energy technologies, Heat and mass transfer < Advanced energy technologies

Performance design of high-temperature chloride salts as thermal energy storage material

Le Zhao[1], Jingyao Wang[1], Liu Cui[1], Baorang Li[1], Xiaoze Du[1,2†], Hongwei Wu[3]

1 Key Laboratory of Power Station Energy Transfer Conversion and System (North China Electric Power University), Ministry of Education, Beijing 102206, China

2 School of Energy and Power Engineering, Lanzhou University of Technology, Lanzhou 730050, China

3 School of Physics, Engineering and Computer Science, University of Hertfordshire, Hatfield, AL109AB, UK

Abstract

The chloride salts have great potential used as high-temperature thermal energy storage (TES) medium for the concentrated solar power system. In this study, a new high-temperature energy storage ternary chloride composed of LiCl, KCl, and $CaCl_2$ was developed based on the phase diagram generated by FactSage. The differential scanning calorimetry (DSC) technique was used to compare the two ternary chloride salts prepared by eutectic composition based on Factsage prediction. The DSC measurements showed that the melting points of these two different components were only 0.46 % and 1.64 % different from those predicted by Factsage. The thermal properties of the two ternary chloride salts were also compared. The solid and liquid-specific heat of

† Corresponding author. Tel.: +86(10)61773923; Fax: +86(10)61773877. Email address: duxz@ncepu.edu.cn (X. Du)

ternary salts was determined by DSC using sapphire as the standard reference. The average specific heat of solid and liquid of salt 1 was 1.46 and 1.79 J/(g·ºC), respectively. The average specific heat of the solid and liquid of salt 2 was 0.73 and 0.95 J/(g·ºC), respectively. The vapor pressure and decomposition temperature of ternary chloride salts were investigated. The results showed that the vapor pressure of salt 1 was almost constant below 650 ºC by FactSage. Meanwhile, the TG results showed that the upper working temperature of salt 1 was 650 °C under the air atmosphere. In addition, the ternary chloride salts after short-term cycling still exhibited excellent thermal properties, which revealed that these good thermal properties make them have broad application prospects in high-temperature thermal energy storage systems.

Key words: Chloride salts; thermal energy storages; thermal properties; thermal stability

Nomenclature

c_p	Specific heat capacity (J/g·ºC)
ΔH	Heat fusion (J/g)
Q	TES density (J/g)
T	Temperature (ºC)
N	The number of tests

Subscripts

a	average
i	initial
l	liquid
max	upper limit working
m	melting
s	solid
xi	Measured values of related paraments
$\bar{x}$	Measured average values of related paraments

1. Introduction

Solar photovoltaic and wind energy forms of renewable energy occupied a very important position in many countries with the electricity market [1]. However, since the intermittent supply of renewable energy, even though the cost of photovoltaic and wind power generation had declined significantly in the past decade, it still pose a great challenge to power grid management [2]. To reduce the load fluctuation of the power grid and prolong its operation time, concentrated solar power (CSP) integrated with thermal energy storage (TES) provides a technology of schedulable renewable power [3].

At present, solar salt ($NaNO_3$–KNO_3 60-40 wt.%) and HITEC ($NaNO_3$–KNO_3–$NaNO_2$ 7-53-40 wt.%) are widely used as TES materials for CSP power plants [4], but the thermal stability and specific heat capacity of these salts still need to be improved. Therefore, to achieve higher energy conversion efficiency and lower standard power cost, the CSP technology with higher TES operating temperature is being developed [5].

Many research groups have screened various components in the multi-component system through a large number of experiments [6-8]. The experimental results showed that the melting point of the nitrate mixture reduced 90 ºC [9]. Quaternary ammonium salt system of $LiNO_3$–$NaNO_3$–KNO_3–$Ca(NO_3)_2$ showed better thermophysical properties than solar salt and HITEC salt in terms of specific heat capacity, thermal stability, and viscosity [10]. Zhao et al. [11] designed and tested ternary nitrates consisted of 50-80 wt.% KNO_3, 0-25 wt.% $LiNO_3$ and 10-45 wt.% $Ca(NO_3)_2$. The experimental results showed that some mixtures exhibited low T_m below 100 ºC. However, its temperature stability only reached 500 ºC. Zhong et al. [12] studied the phase diagram of the $LiNO_3$–KNO_3 system by differential scanning calorimetry and obtained the phase transformation

data of the $LiNO_3$–KNO_3 system. The parameters of all phases and compounds in the $LiNO_3$–$NaNO_3$–KNO_3 nitrate salts also were thermodynamically optimized. $LiNO_3$–$NaNO_3$–KNO_3–$NaNO_2$ nitrate salts were designed to improve energy conversion efficiency based on the thermodynamic calculation of Gibbs fusion energy [13].

The operating temperature of the nitrate system cannot reach the new molten salt TES/heat transfer fluids (HTFs) system (operating temperature range is 520-720 ºC) proposed by NREL [5]. According to the SunShot initiative of DOE, this temperature problem was solved by salts such as carbonate salts, fluoride salts, and chloride salts and their mixtures [5]. Wu et al. [14] mixed Li_2CO_3, K_2CO_3, and Na_2CO_3 in different proportions to prepare 36 kinds of mixed carbonate molten salts. The thermal properties of these 36 kinds of salts were analyzed through experiments. The results showed that the T_m of the main ternary carbonate salts was close to 400 ºC, and the decomposition temperature of most ternary carbonate salts was between 800 ºC and 850 ºC. In 2014, Chen et al. [15] explored the T_m and high-temperature stability of salt mixture of K_2CO_3–Na_2CO_3–Li_2CO_3 through experimental research and thermodynamic model. Further, phase diagrams and thermodynamic properties of 56-44, 25-75, and 75-25 mol.% Na_2CO_3–K_2CO_3 were studied by differential thermal analysis, differential scanning calorimetry, and high-temperature X-ray diffraction (XRD) in 2020 [16]. Differential thermal analysis and differential scanning calorimetry analysis showed that there was a solid-solid transition in a wide temperature range between 375 ºC and 550 ºC. The high-temperature XRD analysis showed that this transformation was a continuous process of unit change, in which the hexagonal lattice structure did not change the cell volume. It is noteworthy that the T_m of carbonate molten salts is relatively high and it is easy to decompose at high temperatures. Consequently, to some extent the large-scale application of

carbonate molten salt materials is limited.

In recent years, Na_2CO_3–NaCl (59.45-40.55 mol.%), Na_2SO_4–NaCl (68.05-31.95 mol.%) and NaF–NaCl–Na_2CO_3 (21.66-41.87-36.47 mol.%) have also been considered as excellent HTFs for the operating temperature of CPS [17-19]. However, these molten salts have high T_m and low TES density, which made these molten salts difficult to replace the existing solar salts and HITEC salts. Unfortunately, the T_m of solar salts and HITEC salts were low, and their corresponding thermal stability was also low. Therefore, molten salts with T_m and high thermal stability are highly important.

In recent years, chloride mixture salts have attracted research from many scholars because of their wide temperature range [20, 21]. Several authors determined that some chloride mixtures could be used as TES/HTFs for the CSP systems [22-26]. The T_m of chloride salt was very low, and the minimum reached 204 ºC [27], but the thermal stability was poor. Wei et al. [20] developed a ternary chloride salt of NaCl, $CaCl_2$, and $MgCl_2$ with a T_m of 424 ºC and solid and liquid C_p of 0.83 and 1.19 J/(g·K), respectively. However, due to the reaction between $MgCl_2$ and water from the atmosphere, it has poor thermal stability under the air atmosphere [28]. At present, the thermal stability of chloride salts with low, and T_m was also low when it was exposed to air. Low thermal stability destroyed the heat storage system and even hindered the heat transfer [29, 30]. Therefore, the research on the molten salt performance of high-temperature TES systems in a wide temperature range is not comprehensive [31]. More studies need to be conducted on the prediction of thermal performance and the evaluation of heat transfer enhancement of chloride salts for high-temperature TES systems.

In addition, the annual production of millions of tons of KCl and low-cost $CaCl_2$ during the

conversion of KCl products in salt lakes in China needs to be consumed. The development of high-temperature heat transfer and storage media with Na, K, Mg, and Ca chloride salts as raw materials are not only expected to break the upper limit of the working temperature of the nitrate molten salt at the maximum of 565 ºC but also possible to realize the resource utilization of salts lake waste salt [32]. However, $CaCl_2$ has a high melting temperature and poor heat transfer performance. In this paper, LiCl with a lower melting temperature and better heat transfer performance is selected to improve thermal performance. The FactSage prediction with experimental verifications was used to obtain the composition and melting temperature of ternary chloride salts of LiCl–KCl–$CaCl_2$. Meanwhile, the main factors for the difference between predicted and actual values are revealed by experiments. Other thermal properties of ternary chloride salts under the two predicted components are compared. The vapor pressure of ternary chloride was predicted by FactSage and its instability mechanism below 700 ºC is revealed. Finally, the thermophysical properties of the ternary chloride salts prepared in this paper will be compared with those of other mixtures to confirm their potential application in high-temperature solar thermal storage.

2. Experiments and methodology

In this paper, ionic compounds of LiCl and KCl with a boiling point higher than 1300 ºC and superior thermal properties were selected. Combined with the covalent chloride $CaCl_2$ with different molecular sizes, shapes, and bonding modes, the ternary chloride was formed in this way. The basic thermophysical properties of these single salts were shown in Table 1. Further, the composition and melting temperature, T_m, of ternary chloride were predicted by FactSage. The Factsage software is a thermochemical modeling software package, which focus on the calculation

and operation of phase diagrams. It can also be used to predict the composition, T_m, chemical properties, and liquid line projection of a wide range of chemical mixtures [31, 33].

Table 1. Detailed thermophysical properties of the selected single chloride salt [34, 35].

Materials	T_m	Temperature boiling	Heat fusion	c_p
	ºC	ºC	J/g	J/mol·K
LiCl	610	1350	416	41.4174 +0.0233969T (298.15 to 2000 K)
KCl	771	1500	353	40.0158+0.0254680T+364,845T^{-2} (298.15 to 2500 K)
$CaCl_2$	775	1934	253	56.3071+0.0293614T +140,210T^{-2} (1045 to 2000 K)

2.1 The prediction of chloride salt's phase diagram

Composition and T_m of ternary chloride salts LiCl–KCl–$CaCl_2$ were predicted by FactSage, as shown in Fig. 2. Different compositions of ternary chloride salts corresponded to different melting temperatures. The ternary chloride salts corresponded to three Tm. In the ternary chloride salts, stable compounds S2 ($KCaCl_3$) and S3 ($KCaCl_3$) were generated in both boundary systems. In the two boundary systems, the corresponding ternary chloride content is different. There are KCl

primary crystals in the S2 region and $CaCl_2$ primary crystals in the S3 region. The temperature that the ternary chloride salts formed a stable compound $KCaCl_3$ under high-temperature conditions will also be different. The predicted T_m and specific components of ternary chloride salts LiCl–KCl–$CaCl_2$ were shown in Table 2. Ternary chloride salts LiCl–KCl–$CaCl_2$ had three different T_m and the corresponding components were different. The chloride salts composition corresponding to T_m of 340.93 ºC was the mass fraction of 37.85-53.38-8.77, and the mass fraction composition corresponding to T_m of 433.57 ºC was 30.90-13.82-55.28. Furthermore, ternary chloride salts LiCl–KCl–$CaCl_2$ with T_m of 626.85 ºC have a corresponding mass fraction of 1.78-18.61-79.61. Since the corresponding T_m under this component was too high, this component was not considered in the following tests. To further determine their corresponding thermal properties, the thermal properties of the two ternary chloride salts were discussed and analyzed in section 3.

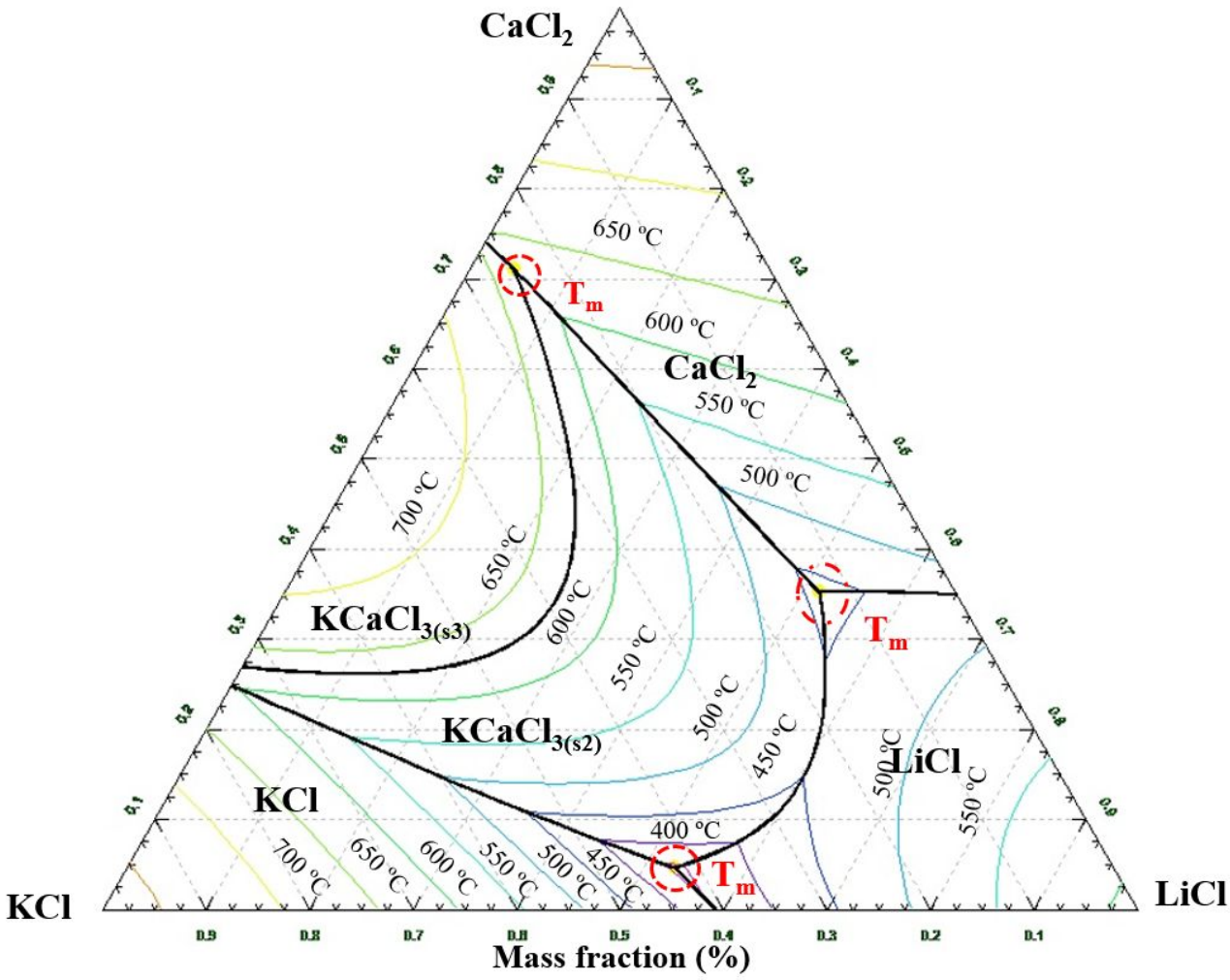

Fig. 1. Phase diagram modeled with FactSage, with the components predicted for ternary chloride salts LiCl–KCl–$CaCl_2$.

Table 2. The predicted T_m and composition of ternary chloride salts LiCl–KCl–$CaCl_2$.

Mixtures	Samples	Proportion	T_m
		wt.%	℃
LiCl–KCl–$CaCl_2$	Salts 1	37.85-53.38-8.77	340.93
	Salts 2	30.90-13.82-55.28	433.57
	Salts 3	1.78-18.61-79.61	626.85

2.2 Materials and synthesis

LiCl (AR, purity ≥ 99.5 %), KCl (AR, purity ≥ 99.5 %), and $CaCl_2$ (AR, purity ≥ 99.0 %) were purchased from Shanghai Macklin Co., Ltd. Unpurified chloride salts were selected for the preparation of the ternary chloride salts. Firstly, the salts were dried in the oven at 120 ºC for 24 h to remove moisture. Then, these salts were fully stirred in a milling bowl according to the predicted molar fraction at room temperature. The mixed salt was heated from room temperature to 700 ºC at a heating rate of 5 ºC/min in a muffle furnace and kept for 30 min to completely melt the KCl. Then, the temperature of the muffle furnace was reduced from 700 to 600 ºC at the rate of 5 ºC/min and kept for 2 h to ensure the complete formation of the eutectic mixture. Finally, the ternary chloride salts were poured into a container and naturally cooled to room temperature.

2.3 Measurements and procedure

A differential scanning calorimeter (DSC 1, Mettler Toledo, Sweden) was used to measure the T_m, heat fusion, and C_p of the ternary chloride salts. Firstly, selecting a lid with holes in the crucible protects the instrument from potential damage [36]. The sample was heated continuously from room temperature to 500 ºC with a heating rate of 10 ºC /min under the argon atmosphere and the flow rate of the gas was maintained at 100 mL/min in the experiments [37]. The temperature error was within ± 0.2 ºC, and the relative error of heat fusion was estimated to be within 2 %. The measurement of C_p was divided into three steps. (a) Blank experiment: The sample and the reference were both empty crucibles. (b) Sapphire experiment: The sample crucible was equipped with a sapphire standard sample, and the reference was an empty crucible. (c) Sample experiment: The sample crucible was filled with ternary chloride salts, and the reference crucible was empty.

Finally, the analysis was carried out with the specific heat software of METTLER TOLEDO DSC. Furthermore, real TES systems should optimally be stable under the air atmosphere. Some researchers have found that the introduction of protective inert gas in the CSP system can reduce the corrosion of metal matrix from chloride salt [37]. Therefore, the thermal stabilities of the chloride salt were measured under the air and argon atmosphere, respectively. A synchronous thermal analyzer (TG-DSC, TGA/DSC3+, Mettler Toledo, Sweden) was used to determine the thermal stability of the chloride salt mixture. The test conditions were that about 5-10 mg of samples were placed in a constant air atmosphere and a constant argon atmosphere. Meanwhile, the heating rate from room temperature to 800 ºC was 10 ºC/min. The temperature error was within ± 0.3 ºC.

Then, the concentration of major impurities in the ternary chloride salts was detected by ICP-OES. Finally, the samples before and after 10 cycles were milled into powder for X-ray diffraction scanning (XRD, Bruker D8 ADVANCE A25X). Accelerating voltage and electric current were 40 kV and 40 mA, respectively. The ternary chloride salts were scanned from 20º to 90º. The thermal stability mechanism of ternary chloride salts was studied by phase analysis of salt 1 and salt 2. In order to ensure the accuracy of the measurement and calculation results during the experiment, Table 3 lists the error sources in this experiment. The error was mainly divided into the error of the experimental device.

Table 3. Instrument accuracy.

Source of error	Error	Error description
Errors in the preparation process	High-temperature muffle furnace	±1 ºC
Experimental device error	Electronic balance	±0.1 %

Temperature (TGA/DSC)	±0.3 ºC
Balance (TGA/DSC)	0.05%
Temperature (DSC)	±0.2 ºC
Heat fusion (DSC)	±2%

3. **Results with analysis**

3.1 Thermal properties analysis

3.1.1 Melting point

The T_m of ternary chloride salts LiCl–KCl–$CaCl_2$ with two different components were determined by DSC, and the DSC heat flow curves in the melting process were shown in Fig. 2. T_m of the ternary chloride salts with a mass fraction of 37.85:53.38:8.77 was 342.51 ºC, which was 1.58 ºC different from the predicted T_m. For this component, the FactSage prediction was quite accurate. However, for the ternary chloride salts with a mass fraction of 30.90:13.82:55.28, there was a large deviation between the observed T_m and the predicted T_m. The experimental T_m was 433.57 ºC, which was 7.13 ºC different from the predicted T_m. To explore the difference between the predicted and experimental T_m, the impurity concentration in the ternary chloride salts LiCl–KCl–$CaCl_2$ was analyzed by ICP-OES, and the results were shown in Table 4. It can be seen from Table 4 that the impurity concentration in salt 1 was much higher than that of salt 2. Therefore, the deviation between the predicted T_m and the experimental T_m was mainly the influence of impurity concentration in salt 1. For salt 2, impurity concentration has a less effect on Tm. The difference between the predicted T_m and the experimental T_m was mainly the high content of calcium chloride, which may be the partial hydrolysis of $CaCl_2$ hydrate. This resulted from the decrease of the

proportion of $CaCl_2$ in the ternary chloride salts and the formation of off-eutectic. To further confirm the main reasons affecting salt 2, we discussed it in detail in section 3.1.3.

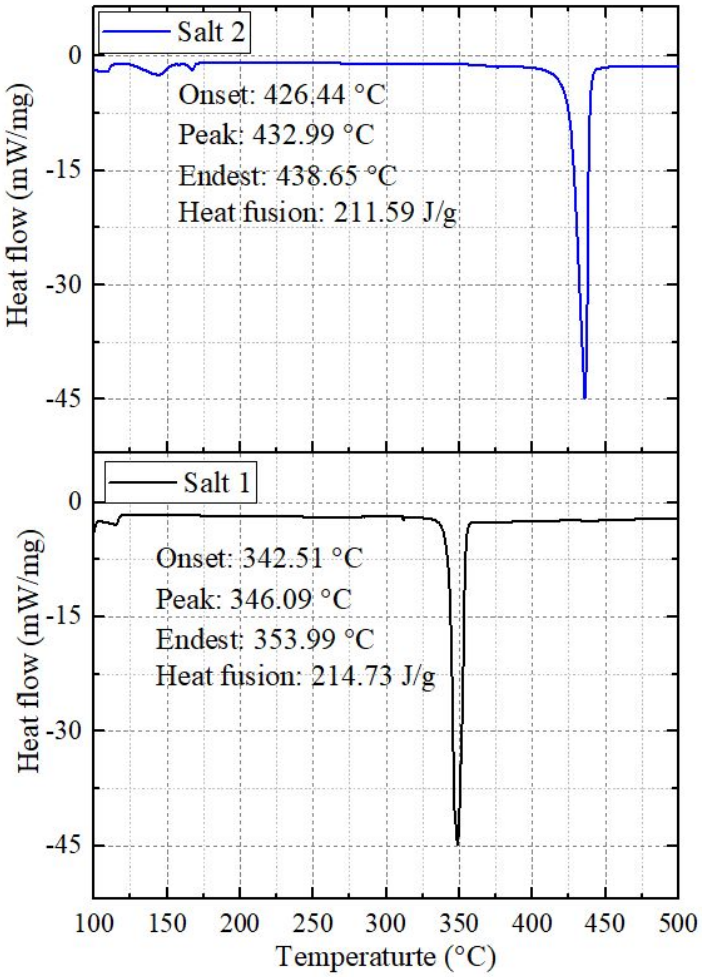

Fig. 2. DSC analysis of ternary chloride salts LiCl–KCl–$CaCl_2$ with different mass fractions under the Ar atmosphere.

Table 4. The concentration of main impurities in ternary chloride salts LiCl–KCl–$CaCl_2$ (mg/kg).

Samples	Cr	Fe	Mn	Ni	Si
Salt 1	15	116	1	3	577
Salt 2	11	73	1	2	341

3.1.2 Specific heat capacity

When the heat storage system operates smoothly, the molten salt after heat absorption is converted into liquid, and the heat storage and heat transfer are continued. Therefore, the C_p and TES density of the ternary chloride salts are also considered to be crucial [37]. The C_p was characterized by the DSC method and drawn in Fig. 3 and the specific data were shown in Table 5. The C_p of salt 1 was divided into solid state (270-320 ºC) and liquid state (450-500 ºC). The C_p of salt 2 also was divided into solid state (330-380 ºC) and liquid state (450-500 ºC). In contrast, the specific heat capacity of liquid salt was relatively stable compared with that of solid salt. It is worth noting that the C_{pl} of the ternary chloride salts liquid was always higher than that of C_{ps}, mainly because of the disorder of liquid ions [20]. The average C_p of solar salt and HITEC were 1.55 J/(g·ºC) and 1.24 J/(g·ºC), respectively [38, 39]. The average C_p of salt 1 was 1.62 J/(g·ºC) higher than that of the above two salts. For the specific heat capacity, ternary chloride salts are comparable to Solar Salt and HITEC, which incate its potential in thermal energy storage.

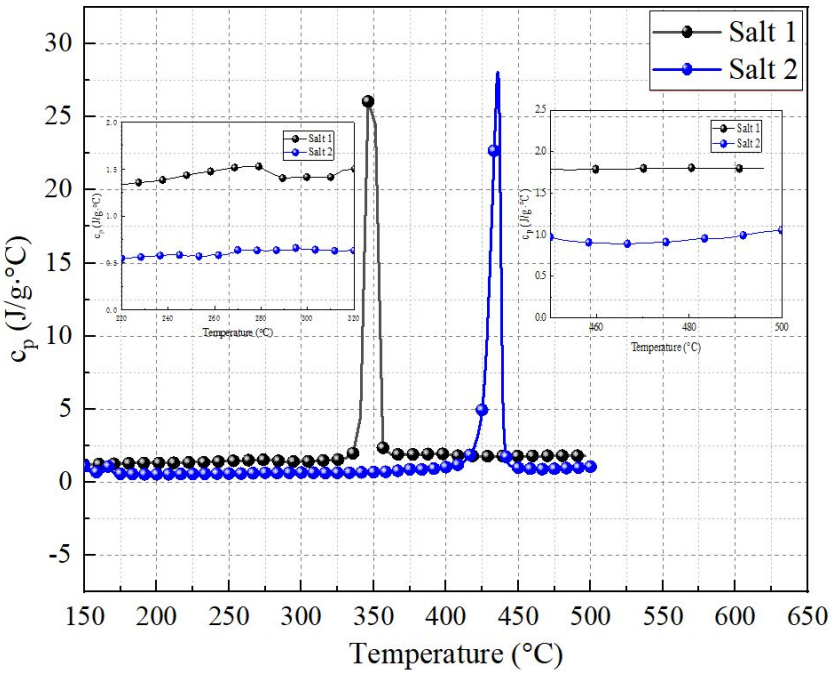

Fig. 3. Specific heat capacity of the chloride salts.

Table 5. C_{ps} and C_{pl} of the ternary chloride salts.

Salt 1				Salt 2			
T	C_{ps}	T	C_{pl}	T	C_{ps}	T	C_{pl}
ºC	J/g·ºC	ºC	J/g·ºC	ºC	J/g·ºC	ºC	J/g·ºC
270	1.52	450	1.78	330	0.64	450	0.97
275	1.53	455	1.78	335	0.64	455	0.92
280	1.53	460	1.78	340	0.66	460	0.90
285	1.46	465	1.78	345	0.67	465	0.88
290	1.41	470	1.80	350	0.68	470	0.90
295	1.41	475	1.80	355	0.69	475	0.91
300	1.42	480	1.80	360	0.72	480	0.94

305	1.42	485	1.80	365	0.76	485	0.96
310	1.41	490	1.80	370	0.84	490	0.98
315	1.49	495	1.79	375	0.88	495	1.02
320	1.50	500	1.80	380	0.86	500	1.06

3.1.3 Thermal stability analysis

Vapor pressure is an important factor to be measured in the TES system. Especially at high temperatures, vapor pressure greater than 1.0 atm poses risks to pipelines and containers [40]. Ternary chloride salts LiCl–KCl–$CaCl_2$ are required to remain stable at high temperatures up to 700 ºC. Therefore, a closed system with a pressure slightly above atmospheric may be required to achieve dynamic vapor-liquid balance and avoid weight loss [41].The vapor pressures of two different components of the ternary chloride salts were simulated by FactSage and the results are shown in Fig. 4. A sharp increase in vapor pressure was observed above 650 ºC, which explains the significant increase in mass loss of the two chloride salts above 650 ºC under an air atmosphere. This result was consistent with the analysis results of the existing literature [42].

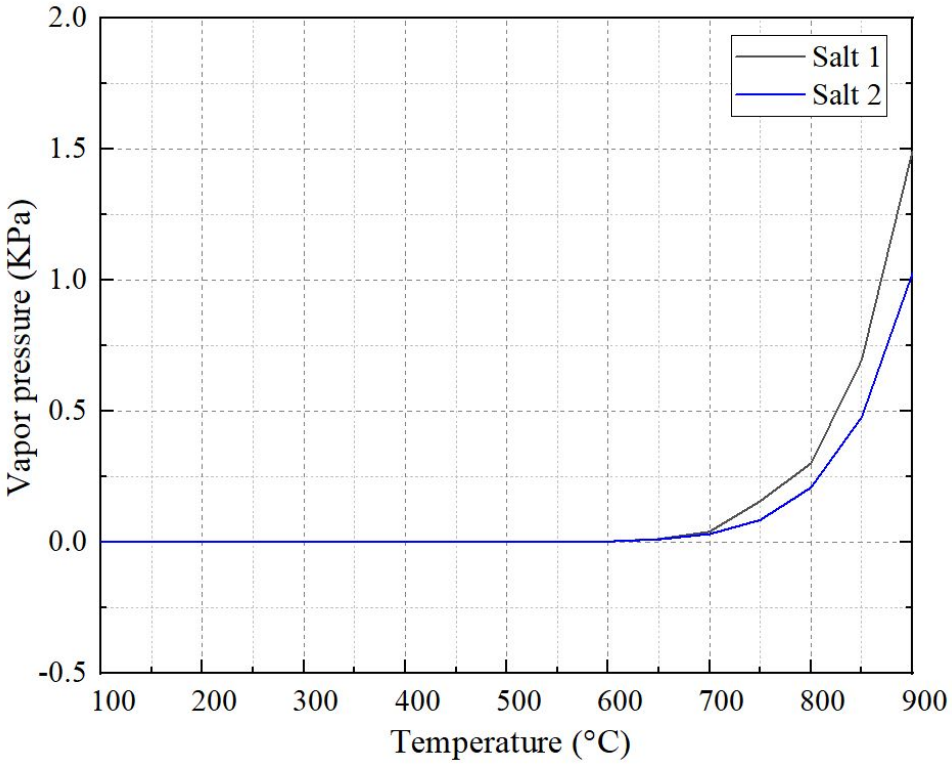

Fig. 4. Vapor pressure of ternary chloride salts LiCl–KCl–$CaCl_2$ predicted using FactSage.

At present, the thermal stability of molten salt is generally determined by TGA and DTG curves. The thermal stability of molten salt is generally defined as the mass loss of molten salt is not more than 3% from solid to liquid [31, 37, 42, 43]. To explore the thermal stability of ternary chloride salts LiCl–KCl–$CaCl_2$ in two kinds of different atmospheres, the thermal stability of salt 1 and salt 2 were evaluated by TGA under the argon and air atmosphere. The TGA and DTG curves after heating were shown in Fig. 5. Fig. 5(a) indicated that salt 1 contained a small amount of water, the first weight loss observed near 100 ºC was about 0.81 % and the second weight loss curve changed sharply after 700 ºC. When the temperature reached 706.5 ºC, the weight loss rate of salt 1 was 3.08 %, and the weight change rate was 0.07006 % /ºC. As shown in the TG curve, the sample mass gradually decreased from about 35 ºC to 120.45 ºC, and the mass loss was 12.31 %, which was the absorption of moisture from ternary chloride salts. This curve indicated that a large amount of

moisture has been evaporated. A small amount of moisture formed $CaCl_2 \cdot nH_2O$ with $CaCl_2$, and it has been hydrolyzed. Another weight loss curve is due to the formation of CaO or $Ca(OH)_2$. The third weight loss curve changed sharply after 700 ºC. At 725 ºC, salt 2 reached the working limit, and the weight loss was 3.04 % with a weight-change rate of 0.05868 %/ºC. Therefore, the optimal working temperature range of salt 1 and salt 2 as HTFs were 150-700 ºC and 310-720 ºC under the argon atmosphere. Fig. 5(b) indicated the weight-change rate of ternary chloride salts LiCl–KCl–$CaCl_2$ under the air atmosphere. Salt 1 evaporated a small amount of $CaCl_2 \cdot 2H_2O$ at 200 ºC until the hydrated salt was completely removed, and the weight change rate at 652 ºC was 0.02374 % / ºC. Therefore, the optimal working temperature range of salt 1 as HTFs was 200-650 ºC under the air atmosphere. In addition, the weight-change rate of salt 2 was 0.00988 %/ºC at 695.5 ºC and the optimal working temperature range of salt 2 as HTFs were 315-690 ºC under the air atmosphere. Therefore, during the heating process of ternary chloride salt, the argon atmosphere can improve the thermal stability of molten salt.

$$CaCl_2 \cdot 6H_2O + \Delta H \leftrightarrow CaCl_2 \cdot 2H_2O + 4H_2O \ 29.9°C: \ 200°C$$

$$CaCl_2 \cdot 2H_2O + \Delta H \leftrightarrow CaCl_2 + 2H_2O \ 260°C$$

$$CaCl_2 + 2H_2O(g) = 2HCl(g) + Ca(OH)_2(s)$$

$$CaCl_2 + H_2O(g) = 2HCl(g) + CaO(s)$$

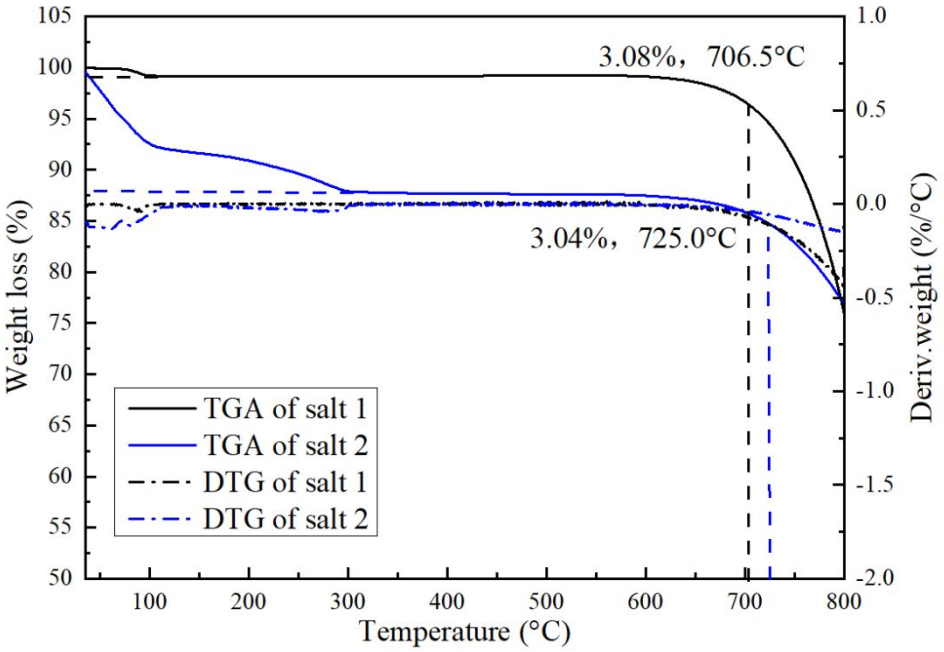

(a) Weight loss curves of salt 1 and salt 2 during the heating process under the argon atmosphere.

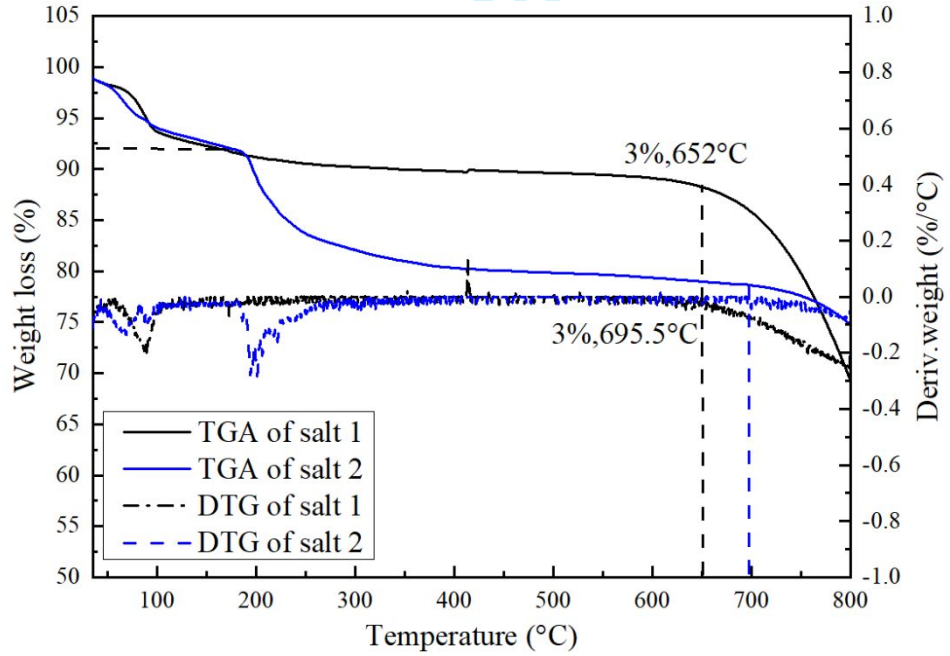

(b) Weight loss curves of salt 1 and salt 2 during the heating process under the air atmosphere.

Fig. 5. Weight loss curves of salt 1 and salt 2 during the heating process under two kinds of different atmospheres.

The phases of the two chloride salts were analyzed by the XRD technique to explore the

instability mechanism of ternary chloride salts up to 700 ℃. Fig. 6 showed the XRD patterns of salt 1 and salt 2. It can be seen that there is no other by-products produced in salt 1, but salt 2 produced $CaCl_2 \cdot nH_2O$ due to its high $CaCl_2$ content and strong moisture absorption. Therefore, by-products generated at high temperatures due to the hydrolysis of $CaCl_2$ in salt 2. This may also lead to an error between the predicted T_m and the experimental T_m.

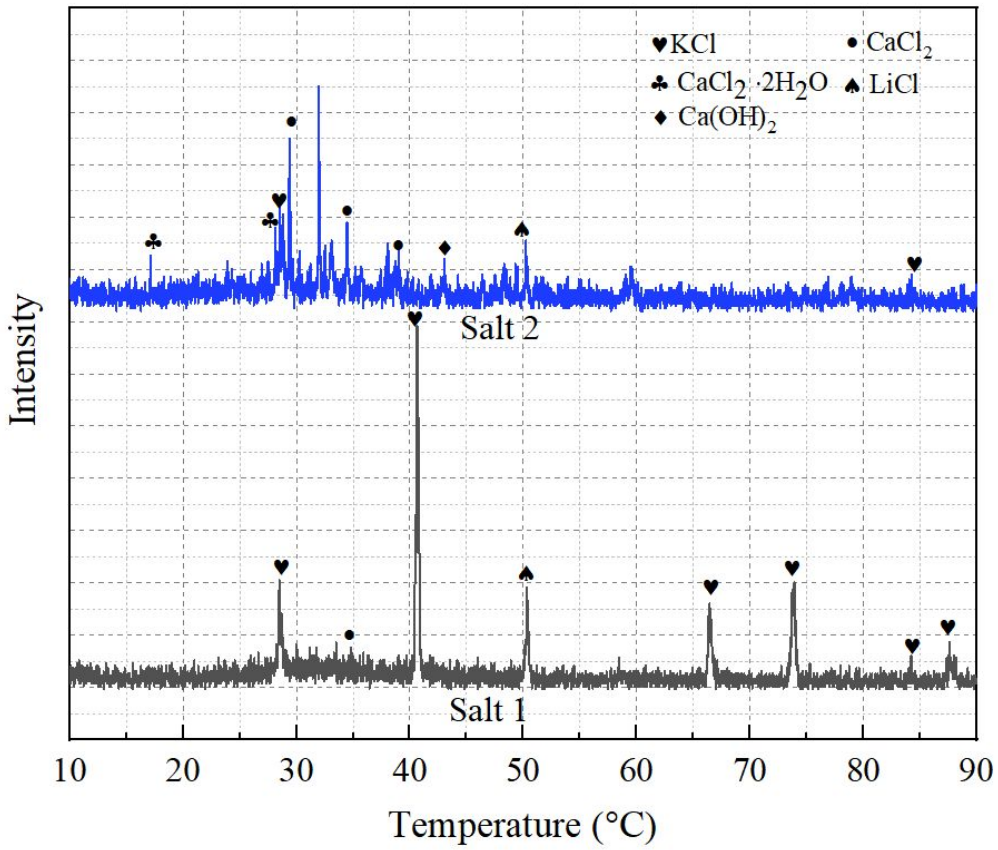

Fig. 6. The XRD of the ternary chloride salts with different components.

3.1.4 TES density analysis

Fig. 2 showed that the heat fusion of Salt 1 and Salt 2 were 214.73 J/g and 211.59 J/g, respectively. Salt 1 and Salt 2 can store huge energy during the phase transition process, which was very suitable for high-temperature solar energy storage. Further, the capacity and efficiency of storage of molten salt used in thermal energy were directly determined by TES density. The heat

fusion and sensible heat of molten salt were included, which can be calculated by following Eq. (1) [44, 45]

$$Q = \int_{Ti}^{Tm} Cp_{sa} + \Delta H + \int_{Tm}^{T\max} Cp_{la} \qquad (1)$$

where Q was TES density; T_i, T_m, and T_l were the initial temperature, T_{max} and the upper limit working temperature for molten salt; C_{ps} and C_{pla} were the solid and liquid specific heat capacity for the ternary chloride salts, respectively; ΔH was the heat fusion.

In this work, when ternary chloride salts are used as TES material. Under argon and air atmospheres, the water removal of salt 1 is completed at 200 °C, and the decomposition of salt 2 is completed at 310 °C. Therefore, the range of 200 ºC to 700 ºC and the range of 310 ºC to 720 ºC were selected as the working temperature for salt 1 and salt 2 under argon atmosphere, respectively, as shown in Fig. 7. The TES density of salt 1 was 1033.23 MJ/m^3, in which the sensible heat capacity and the heat fusion account for 79.22 % and 20.78 % of TES density, respectively. The TES density of salt 2 was 562.64 MJ/m^3, in which the sensible heat capacity and heat fusion account for 62.39 % and 37.61 % of TES density, respectively. Meanwhile, TES density under the air atmosphere was shown in Fig.4. Due to the strong water absorption of $CaCl_2$, $CaCl_2$ formed $CaCl_2 \cdot 2H_2O$ under the air atmosphere from room temperature to 200 ºC. Therefore, the range of 200 ºC to 650 ºC and the range of 315 ºC to 690 ºC were selected as the working temperature under the air atmosphere. The TES density of salt 1 was 944.23 MJ/m^3, in which the sensible heat capacity and the heat fusion account for 77.26 % and 22.74 % of TES density under the air atmosphere, respectively. The TES density of salt 2 was 525.74 MJ/m^3. The TES density of salt 1 is much higher than that of salt 2 under both air and argon atmosphere. In addition, the TES density of the ternary chloride salts was compared with that of two typical commercial solar salt and HITEC

salt [46, 47]. The TES densities of solar salt and HITEC salt are 756.02 and 1080 MJ/m3, respectively. Salt 1 showed excellent TES density (24.9 % higher than solar salt and 14.4 % lower than HITEC salt under the air atmosphere). Low T_m and high TES density indicated that salt 1 exhibited higher potential in high-temperature TES and transfer applications [43].

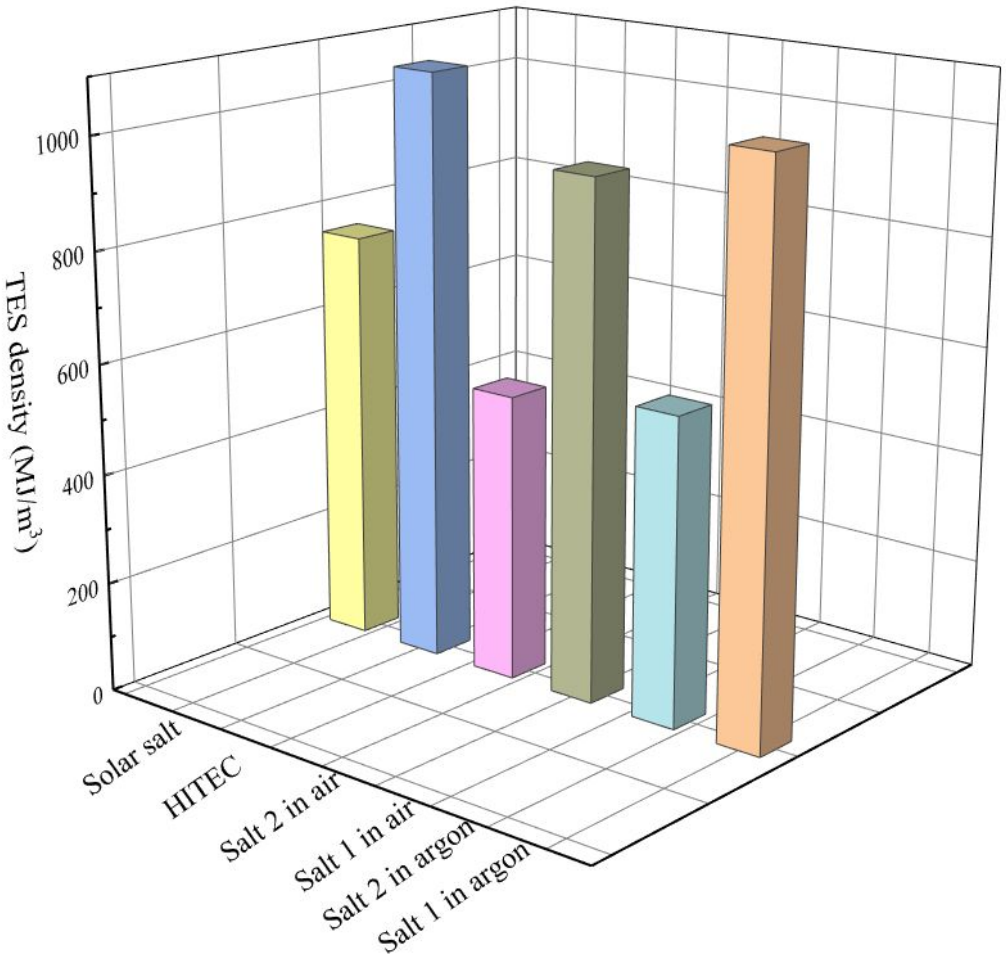

Fig. 7. TES density of the nitrate salts and ternary chloride salts.

3.2 Thermal properties analysis after cycling

It is essential that the potential thermal storage material can be reused and its corresponding properties such as T_m should remain stable after recycling. The thermal storage properties of salt 1 and salt 2 were cycled 10 times at 200 ~ 750 ºC. The results were shown in Fig.8. It can be seen from the heating curves that the T_m of salt 1 remained around 341 ºC, which was consistent with the

DSC test results. After 10 thermal cycles, the T_m of salt 2 increased by 4.50 ℃, which was the release of calcium ions due to the reduction of crystal water, so the cycled salt 2 was close to the predicted T_m. In addition, the two salts had a melting peak of around 175 ℃ due to the melting reaction of the calcium chloride crystal water after 10 cycles during the cycle. Further, after cycling the heat fusion of the two salts decreased inordinately, with a decreasing rate of salt 1 and salt 2 of 9.31 J/g and 5.63 J/g, respectively.

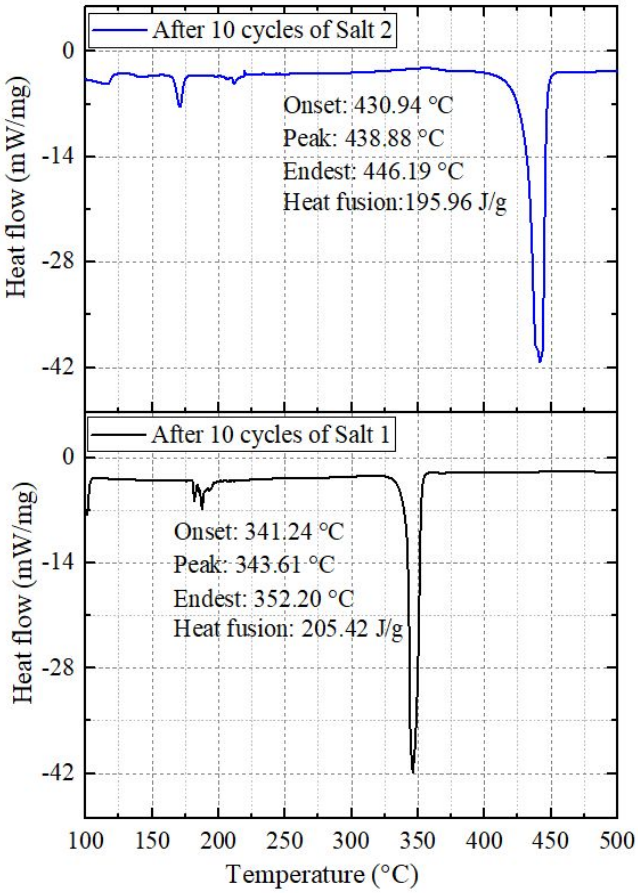

Fig. 8. DSC curves of the ternary chloride salts after 10 thermal cycles.

Fig. 9 showed the XRD pattern of the ternary chloride salts after 10 cycles. With the extension of heating time, the change of composition can be observed. However, the change was only observed in the composition of $CaCl_2 \cdot H_2O$.Therefore, it can be concluded that because of the strong

hygroscopicity of $CaCl_2$ during sample loading, $CaCl_2$ absorbed a small amount of moisture to form calcium chloride-containing crystal water. $CaCl_2$-containing crystal water was continuously decomposed during the high-temperature cycle, which was the main reason for the thermal instability of the ternary chloride salts. Salt 1 had fewer decomposition components on account of its little content of $CaCl_2$. However, salt 2 had relatively more $CaCl_2$, so it broke down a variety of calcium-containing products during high-temperature cycling [48].

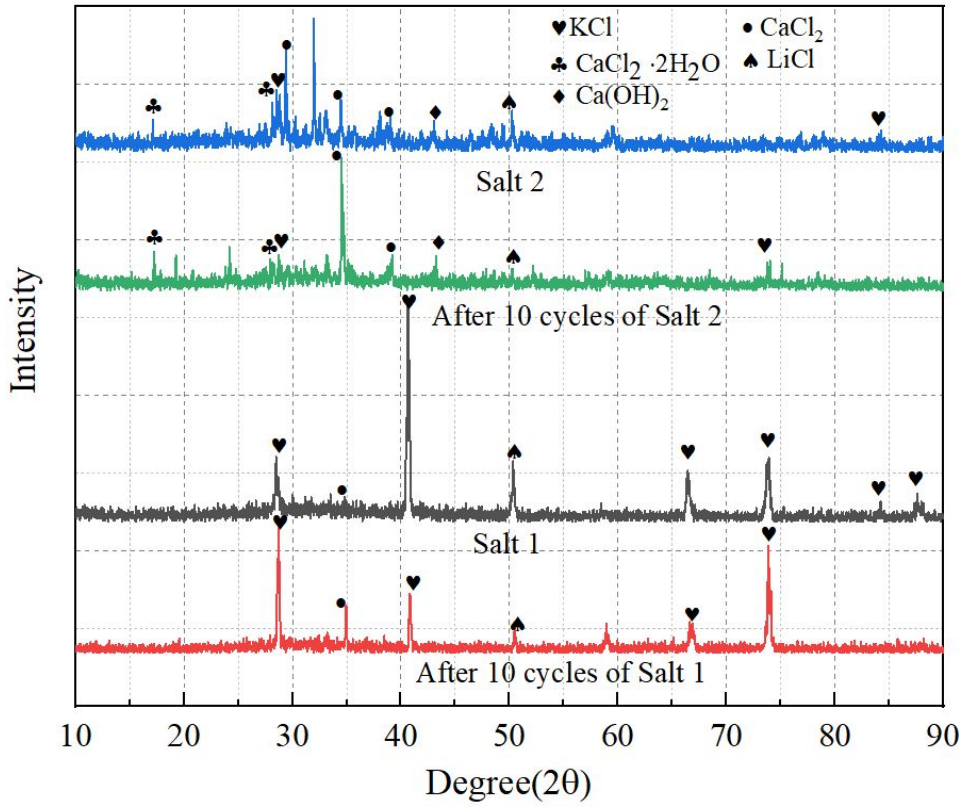

Fig. 9. XRD patterns of the ternary chloride salts before and after cycles.

3.3 Error analysis

To verify the accuracy of the experiment, this paper has analyzed the experimental errors caused by instruments, environment, and reading. During the experiment, the standard deviation of related parameters for salt 1 is calculated by Eq. (2) [26],

$$S_{\bar{x}}=S_x/\sqrt{N} \quad (2)$$

Further, the standard deviation of the mean value is expressed as:

$$S_x=\sqrt{\sum_{i=1}^{N}(M_{xi}-\overline{M_x})^2/(N-1)} \quad (3)$$

where xi and $\bar{x}$ are the measured values and average values of related paraments, respectively, and N is the number of tests.

In this paper, the temperature, heat fusion, and C_p of salt 1 were measured, respectively. Their instrument-related errors have been shown in Table 3. Each experiment was repeated three times. The standard deviations of the mean values for temperature (including onset temperature and thermal stability), heat fusion, C_p and TES density during the whole experiment was shown in Table 6.

Table 6. Error analysis results.

Parameter	Standard deviation
T_m	0.635 °C
C_{ps}	0.064 J/g·°C
C_{pl}	0.155 J/g·°C
ΔH	2.235 J/g
TES density	14.290 MJ/m3
Thermal stability	0.420 °C

3.4 Comparison with other works

In this section, we presented a comparison of the thermal properties obtained in this study with other literature, as shown in Table 7. Han et al. [31] prepared high-temperature TES materials using

$MgCl_2$:KCl: NaCl with a molar ratio of 51:22:27. The experimental results showed that the T_m was 399.7 ºC, and the average $C_{p\text{-}s}$ and $C_{p\text{-}l}$ were 0.90 and 1.13 J/(g·ºC), respectively. These samples could work at operating temperature up to 700 ºC under the argon atmosphere. Du et al. [37] designed a potential candidate for high-temperature TES ($NaCl–CaCl_2–MgCl_2$) applications up to 650 ºC under the argon atmosphere. The thermal properties of these chlorides were experimentally measured. The experimental results showed that the T_m of $NaCl–CaCl_2–MgCl_2$ was 420.83 ºC, and the average $C_{p\text{-}s}$ and $C_{p\text{-}l}$ were 1.43 and 1.47 J/(g·ºC), respectively. Although $NaCl–KCl–ZnCl_2$ has been proven to have a lower T_m of 229 ºC, its thermal stability was far less than the 700 ºC required by the third generation of TES materials [26].

In addition, the ternary chlorides prepared in this study were compared with different mixed salts and nitrate salts. Li et al. [49] prepared a 50 wt. % $LiNO_3$-45 wt. % $NaNO_3$-5 wt.% KCl ternary mixed molten salt by the static mixed melting method. The experimental results showed that the T_m of ternary mixed salt was 172.4 ºC and the heat fusion was 267.9 J/g. To get a lower T_m, Wu et al. [50] prepared 19 different proportions of binary mixed molten salts. The results showed that $KNO_3–Ca(NO_3)_2·4H_2O$ had a low T_m and high thermal stability. The T_m of the selected binary salt mixture was determined to be 116.9 ºC, and the thermal stability was as high as 569.7 ºC.

To further explore the thermal properties of chlorides, ternary chlorides were prepared in this study, with a T_m of 336.64 ºC and average c_{psa} and c_{pla} of 1.46 and 1.79 J/(g·ºC), respectively, which have good heat capacity in the working temperature range. More gratifying is that it can be operated within the working range of up to 650 ºC and 700 ºC in air and argon atmosphere, respectively.

Table 7. Comparison of thermal properties of chloride salts in this study with those in the existing literature.

Samples	T_m	C_p		Thermal stability under a different atmosphere	Reference
		Solid	Liquid		
	ºC	J/(g·ºC)		ºC	
$NaCl–KCl–MgCl_2$	399.7	0.90	1.13	>700 under argon	[31]
$NaCl–CaCl_2–MgCl_2$	420.83	1.43	1.47	650 under argon	[37]
$NaCl–KCl–ZnCl_2$	229 .00	/	0.90	400 under air	[26]
$LiNO_3–NaNO_3–KCl$	172.40	/	/	550 under N_2	[49]
KNO3–$Ca(NO3)_2 \cdot 4H_2O$	116.90	/	1.50	569.7	[50]
$LiCl–KCl–CaCl_2$	342.51	1.46	1.79	650 under air	This study

4. Conclusion

In this study, the melting temperature, composition, and corresponding vapor pressure of ternary chloride salts $LiCl–KCl–CaCl_2$ were predicted. The thermal properties as well as the thermal stability of ternary chloride salts $LiCl–KCl–CaCl_2$ were studied through experiments. The following conclusions can be drawn.

(1) The melting temperature, T_m, and corresponding composition of ternary chloride salts $LiCl–KCl–CaCl_2$ were predicted and tested respectively. The results showed that the predicted and experimental T_m of ternary chloride salts $LiCl–KCl–CaCl_2$ with the mass fraction of 37.847:53.378:8.775 were 340.93 ºC and 342.51 ºC, respectively. The corresponding C_{ps} and C_{pl} were 1.46 and 1.79 J / g·ºC, respectively, the thermal stability was 650 ºC and the TES density was

944.23 MJ/m^3 under the air atmosphere. Moreover, the predicted and experimental T_m of ternary chloride salts LiCl–KCl–$CaCl_2$ with the mass fraction of 30.900:13.822:55.28 were 433.57 ºC and 438.65 ºC, respectively. The corresponding C_{ps} and C_{pl} were 0.73 and 0.95 J / g·ºC, respectively, the thermal stability was nearly 700 ºC and the TES density was 525.74.29 MJ/m^3 under the air atmosphere.

(2) Two chloride salts showed excellent thermal properties, especially the ternary chloride salts with a mass fraction of 30.900:13.822:55.278. Furthermore, it also showed excellent thermal stability above 650 ºC. The optimal working temperature range of both the ternary chloride salt as HTFs were 200-700 ºC under the argon atmosphere and 315-650 ºC under the air atmosphere.

(3) After ten high-temperature thermal cycles, ternary chloride salts LiCl–KCl–$CaCl_2$ still showed good thermal performance. After cycling, salt 1 was maintained at about 341 ºC, and the heat fusion decreased by 9.31 J/g. The T_m of salt 2 increased by 4.5 ºC, but the difference with the predicted T_m was only 2.63 ºC. The heat fusion decreased by 15.63 J/g.

(4) From the X-ray diffraction analysis, the thermal instability factor was confirmed to be the strong moisture absorption of $CaCl_2$, forming $CaCl_2 \cdot H_2O$ and decomposing into various by-products.

Acknowledgements

This work was financially supported by the National Natural Science Foundation of China (Grant No. 52130607, 52090062 and 52211530087) and the Double First-Class Key Program of Gansu Provincial Department of Education (Grant No. GCJ2022-38)

References

[1] M. Liu, E.S. Omaraa, J. Qi, P. Haseli, J. Ibrahim, D. Sergeev, M. Müller, F. Bruno, P. Majewski, Review and characterisation of high-temperature phase change material candidates between 500 C and 700°C, Renewable and Sustainable Energy Reviews 150 (2021) 111528. https://doi.org/10.1016/j.rser.2021.111528.

[2] Y. Kumar, J. Ringenberg, Soma S. Depuru, V.K. Devabhaktuni, Jin W. Lee, E. Nikolaidis, B. Andersen, A. Afjeh, Wind energy: Trends and enabling technologies, Renewable and Sustainable Energy Reviews 53 (2016) 209-224. https://doi.org/10.1016/j.rser.2015.07.200.

[3] W. Ding, A. Bonk, T. Bauer, Corrosion behavior of metallic alloys in molten chloride salts for thermal energy storage in concentrated solar power plants: A review, Frontiers of Chemical Science and Engineering 12 (2018) 564-576. https://doi.org/10.1007/s11705-018-1720-0.

[4] M. Liu, N.H. Steven Tay, S. Bell, M. Belusko, R. Jacob, G. Will, W. Saman, F. Bruno, Review on concentrating solar power plants and new developments in high temperature thermal energy storage technologies, Renewable and Sustainable Energy Reviews 53 (2016) 1411-1432. https://doi.org/10.1016/j.rser.2015.09.026.

[5] M. Mehos, C. Turchi, J. Gomez-Vidal, M. Wagner, Z. Ma, C. Ho, W. Kolb, C. Andraka, A. Kruizenga, Concentrating Solar Power Gen3 Demonstration Roadmap, 2017.

[6] J. Lee, B. Jo, Nanoencapsulation of binary nitrate molten salts for thermal energy storage: Synthesis, thermal performance, and thermal reliability, Solar Energy Materials and Solar Cells 230 (2021) 111284. https://doi.org/10.1016/j.solmat.2021.111284.

[7] T. Delise, A.C. Tizzoni, C. Menale, M.T.F. Telling, R. Bubbico, T. Crescenzi, N. Corsaro, S. Sau, S. Licoccia, Technical and economic analysis of a CSP plant presenting a low freezing ternary

mixture as storage and transfer fluid, Applied Energy 265 (2020) 114676. https://doi.org/10.1016/j.apenergy.2020.114676.

[8] A.G. Fernández, S. Ushak, H. Galleguillos, F.J. Pérez, Thermal characterisation of an innovative quaternary molten nitrate mixture for energy storage in CSP plants, Solar Energy Materials and Solar Cells 132 (2015) 172-177. https://doi.org/10.1016/j.solmat.2014.08.020.

[9] N. Ren, Y.-t. Wu, C.-f. Ma, L.-x. Sang, Preparation and thermal properties of quaternary mixed nitrate with low melting point, Solar Energy Materials and Solar Cells 127 (2014) 6-13. https://doi.org/10.1016/j.solmat.2014.03.056.

[10] A.G. Fernández, S. Ushak, H. Galleguillos, F.J. Pérez, Development of new molten salts with LiNO3 and Ca(NO3)2 for energy storage in CSP plants, Applied Energy 119 (2014) 131-140. https://doi.org/10.1016/j.apenergy.2013.12.061.

[11] C.Y. Zhao, Z.G. Wu, Thermal property characterization of a low melting-temperature ternary nitrate salt mixture for thermal energy storage systems, Solar Energy Materials and Solar Cells 95 (2011) 3341-3346. https://doi.org/10.1016/j.solmat.2011.07.029.

[12] Y. Zhong, H. Yang, M. Wang, Thermodynamic evaluation and optimization of LiNO3–KNO3–NaNO3 ternary system, Calphad 71 (2020) 102202. https://doi.org/10.1016/j.calphad.2020.102202.

[13] T. Wang, D. Mantha, R.G. Reddy, Novel low melting point quaternary eutectic system for solar thermal energy storage, Applied Energy 102 (2013) 1422-1429. https://doi.org/10.1016/j.apenergy.2012.09.001.

[14] Y.T. Wu, N. Ren, T. Wang, C. F. Ma, Experimental study on optimized composition of mixed carbonate salt for sensible heat storage in solar thermal power plant, Solar Energy 85 (2011) 1957-

1966. https://doi.org/10.1016/j.solener.2011.05.004.

[15] C. Chen, T. Tran, R. Olivares, S. Wright, S. Sun, Coupled Experimental Study and Thermodynamic Modeling of Melting Point and Thermal Stability of Li2CO3-Na2CO3-K2CO3 Based Salts, Journal of Solar Energy Engineering 136 (2014) https://doi.org/10.1115/1.4027264.

[16] D. Sergeev, E. Yazhenskikh, P. Haseli, M. Liu, M. Ziegner, F. Bruno, M. Müller, Experimental study of thermodynamic properties and phase equilibria in Na2CO3–K2CO3 system, Calphad 71 (2020) 101992. https://doi.org/10.1016/j.calphad.2020.101992.

[17] X. Li, S. Wu, Y. Wang, L. Xie, Experimental investigation and thermodynamic modeling of an innovative molten salt for thermal energy storage (TES), Applied Energy 212 (2018) 516-526. https://doi.org/10.1016/j.apenergy.2017.12.069.

[18] Y. Jiang, Y. Sun, R.D. Jacob, F. Bruno, S. Li, Novel Na2SO4-NaCl-ceramic composites as high temperature phase change materials for solar thermal power plants (Part I), Solar Energy Materials and Solar Cells 178 (2018) 74-83. https://doi.org/10.1016/j.solmat.2017.12.034.

[19] Y. Jiang, Y. Sun, M. Liu, F. Bruno, S. Li, Eutectic Na2CO3–NaCl salt: A new phase change material for high temperature thermal storage, Solar Energy Materials and Solar Cells 152 (2016) 155-160. https://doi.org/10.1016/j.solmat.2016.04.002.

[20] X. Wei, M. Song, W. Wang, J. Ding, J. Yang, Design and thermal properties of a novel ternary chloride eutectics for high-temperature solar energy storage, Applied Energy 156 (2015) 306-310. https://doi.org/10.1016/j.apenergy.2015.07.022.

[21] X. Wei, M. Song, Q. peng, J. Ding, J. Yang, Quaternary Chloride Eutectic Mixture for Thermal Energy Storage at High Temperature, Energy Procedia 75 (2015) 417-422. https://doi.org/10.1016/j.egypro.2015.07.407.

[22] K. Vignarooban, X. Xu, A. Arvay, K. Hsu, A.M. Kannan, Heat transfer fluids for concentrating solar power systems – A review, Applied Energy 146 (2015) 383-396. https://doi.org/10.1016/j.apenergy.2015.01.125.

[23] X. Li, N. Li, W. Liu, Z. Tang, J. Wang, Unrevealing the thermophysical properties and microstructural evolution of MgCl2–NaCl–KCl eutectic: FPMD simulations and experimental measurements, Solar Energy Materials and Solar Cells 210 (2020) 110504. https://doi.org/10.1016/j.solmat.2020.110504.

[24] P.D. Myers, D.Y. Goswami, Thermal energy storage using chloride salts and their eutectics, Applied Thermal Engineering 109 (2016) 889-900. https://doi.org/10.1016/j.applthermaleng.2016.07.046.

[25] X. Wang, J.D. Rincon, P. Li, Y. Zhao, J. Vidal, Thermophysical properties experimentally tested for NaCl-KCL-MgCl2eutectic molten salt as a next-generation high-temperature heat transfer fluids in concentrated solar power systems, Journal of Solar Energy Engineering, Transactions of the ASME 143 (2021) https://doi.org/10.1115/1.4049253.

[26] X. Xu, G. Dehghani, J. Ning, P. Li, Basic properties of eutectic chloride salts NaCl-KCl-ZnCl2 and NaCl-KCl-MgCl2 as HTFs and thermal storage media measured using simultaneous DSC-TGA, Solar Energy 162 (2018) 431-441. https://doi.org/10.1016/j.solener.2018.01.067.

[27] P. Li, E. Molina, K. Wang, X. Xu, G. Dehghani, A. Kohli, Q. Hao, M.H. Kassaee, S.M. Jeter, A.S. Teja, Thermal and Transport Properties of NaCl–KCl–ZnCl2 Eutectic Salts for New Generation High-Temperature Heat-Transfer Fluids, Journal of Solar Energy Engineering 138 (2016) https://doi.org/10.1115/1.4033793.

[28] Q. Huang, G. Lu, J. Wang, J. Yu, Thermal decomposition mechanisms of MgCl2·6H2O and

MgCl2·H2O, Journal of Analytical and Applied Pyrolysis 91 (2011) 159-164. https://doi.org/10.1016/j.jaap.2011.02.005.

[29] J.-w. Wang, C.-z. Zhang, Z.-h. Li, H.-x. Zhou, J.-x. He, J.-c. Yu, Corrosion behavior of nickel-based superalloys in thermal storage medium of molten eutectic NaCl-MgCl2 in atmosphere, Solar Energy Materials and Solar Cells 164 (2017) 146-155. https://doi.org/10.1016/j.solmat.2017.02.020.

[30] K. Vignarooban, X. Xu, K. Wang, E.E. Molina, P. Li, D. Gervasio, A.M. Kannan, Vapor pressure and corrosivity of ternary metal-chloride molten-salt based heat transfer fluids for use in concentrating solar power systems, Applied Energy 159 (2015) 206-213. https://doi.org/10.1016/j.apenergy.2015.08.131.

[31] D. Han, B. Guene Lougou, Y. Xu, Y. Shuai, X. Huang, Thermal properties characterization of chloride salts/nanoparticles composite phase change material for high-temperature thermal energy storage, Applied Energy 264 (2020) 114674. https://doi.org/10.1016/j.apenergy.2020.114674.

[32] Xiaolan Wei, Pei Xie, Weilong Wang, Jianfeng Lu, J. Ding, Calculation of phase diagram and thermal stability of molten salt for ternary chloride systems containing calcium, CIESC Journal 72 (2021) https://doi.org/10.11949/0438-1157.20201710.

[33] C.W. Bale, P. Chartrand, S.A. Degterov, G. Eriksson, K. Hack, R. Ben Mahfoud, J. Melançon, A.D. Pelton, S. Petersen, FactSage thermochemical software and databases, Calphad 26 (2002) 189-228. https://doi.org/10.1016/S0364-5916(02)00035-4.

[34] C. Robelin, P. Chartrand, Thermodynamic evaluation and optimization of the (NaCl+KCl+MgCl2+CaCl2+ZnCl2) system, The Journal of Chemical Thermodynamics 43 (2011) 377-391. https://doi.org/10.1016/j.jct.2010.10.013.

[35] M.M. Kenisarin, High-temperature phase change materials for thermal energy storage, Renewable and Sustainable Energy Reviews 14 (2010) 955-970. https://doi.org/10.1016/j.rser.2009.11.011.

[36] Y. Hu, Y. He, Z. Zhang, D. Wen, Effect of Al2O3 nanoparticle dispersion on the specific heat capacity of a eutectic binary nitrate salt for solar power applications, Energy Conversion and Management 142 (2017) 366-373. https://doi.org/10.1016/j.enconman.2017.03.062.

[37] L. Du, J. Ding, H. Tian, W. Wang, X. Wei, M. Song, Thermal properties and thermal stability of the ternary eutectic salt NaCl-CaCl2-MgCl2 used in high-temperature thermal energy storage process, Applied Energy 204 (2017) 1225-1230. https://doi.org/10.1016/j.apenergy.2017.03.096.

[38] T. Bauer, N. Pfleger, N. Breidenbach, M. Eck, D. Laing, S. Kaesche, Material aspects of Solar Salt for sensible heat storage, Applied Energy 111 (2013) 1114-1119. https://doi.org/10.1016/j.apenergy.2013.04.072.

[39] N. Boerema, G. Morrison, R. Taylor, G. Rosengarten, Liquid sodium versus Hitec as a heat transfer fluid in solar thermal central receiver systems, Solar Energy 86 (2012) 2293-2305. https://doi.org/10.1016/j.solener.2012.05.001.

[40] X. Xu, X. Wang, P. Li, Y. Li, Q. Hao, B. Xiao, H. Elsentriecy, D. Gervasio, Experimental Test of Properties of KCl–MgCl 2 Eutectic Molten Salt for Heat Transfer and Thermal Storage Fluid in Concentrated Solar Power Systems, Journal of Solar Energy Engineering 140 (2018) 051011. https://doi.org/10.1115/1.4040065.

[41] G. Mohan, M. Venkataraman, J. Gomez-Vidal, J. Coventry, Thermo-economic analysis of high-temperature sensible thermal storage with different ternary eutectic alkali and alkaline earth metal chlorides, Solar Energy 176 (2018) 350-357. https://doi.org/10.1016/j.solener.2018.10.008.

[42] G. Mohan, M. Venkataraman, J. Gomez-Vidal, J. Coventry, Assessment of a novel ternary eutectic chloride salt for next generation high-temperature sensible heat storage, Energy Conversion and Management 167 (2018) 156-164. https://doi.org/10.1016/j.enconman.2018.04.100.

[43] H. Tian, W. Wang, J. Ding, X. Wei, Thermal performance and economic evaluation of NaCl–CaCl2 eutectic salt for high-temperature thermal energy storage, Energy 227 (2021) 120412. https://doi.org/10.1016/j.energy.2021.120412.

[44] Y.B. Tao, C.H. Lin, Y.L. He, Preparation and thermal properties characterization of carbonate salt/carbon nanomaterial composite phase change material, Energy Conversion and Management 97 (2015) 103-110. https://doi.org/10.1016/j.enconman.2015.03.051.

[45] A. Awad, H. Navarro, Y. Ding, D. Wen, Thermal-physical properties of nanoparticle-seeded nitrate molten salts, Renewable Energy 120 (2018) 275-288. https://doi.org/10.1016/j.renene.2017.12.026.

[46] H.A. Aljaerani, M. Samykano, A.K. Pandey, K. Kadirgama, R. Saidur, Thermo-physical properties and corrosivity improvement of molten salts by use of nanoparticles for concentrated solar power applications: A critical review, Journal of Molecular Liquids 314 (2020) 113807. https://doi.org/10.1016/j.molliq.2020.113807.

[47] X. Xiao, H. Jia, S. Pervaiz, D. Wen, Molten Salt/Metal Foam/Graphene Nanoparticle Phase Change Composites for Thermal Energy Storage, ACS Applied Nano Materials 3 (2020) 5240-5251. https://doi.org/10.1021/acsanm.0c00648.

[48] L.M. Uriarte, J. Dubessy, P. Boulet, V.G. Baonza, I. Bihannic, P.J.J.o.R.S.A.I.J.f.O.W.i.A.A.o.R.S. Robert, Including Higher Order Processes,, A. Brillouin-, R. Scattering, Reference Raman spectra of synthesized CaCl2 center dot nH(2)O solids (n=0, 2, 4, 6),

(2015)

[49] Y. Li, G. Yue, Y.M. Yu, Q.Z. Zhu, Preparation and thermal characterization of LiNO3–NaNO3–KCl ternary mixture and LiNO3–NaNO3–KCl/EG composites, Energy 196 (2020) 117067. https://doi.org/10.1016/j.energy.2020.117067.

[50] Y. T. Wu, Y. Li, Y. W. Lu, H. F. Wang, C. F. Ma, Novel low melting point binary nitrates for thermal energy storage applications, Solar Energy Materials and Solar Cells 164 (2017) 114-121. https://doi.org/10.1016/j.solmat.2017.02.021.

Table captions

Table 1. Detailed thermophysical properties of the selected single chloride salt [34, 35].

Table 2. The predicted T_m and composition of ternary chloride salts LiCl–KCl–$CaCl_2$.

Table 3. Instrument accuracy.

Table 4. The concentration of main impurities in ternary chloride salts LiCl–KCl–$CaCl_2$ (mg/kg).

Table 5. C_{ps} and C_{pl} of the ternary chloride salts.

Table 6. Error analysis.

Table 7. Comparison of thermal properties of chloride salts in this study with those in the existing literature.

Figure captions

Fig. 1. Phase diagram modeled with FactSage, with the components predicted for ternary chloride salts LiCl–KCl–$CaCl_2$.

Fig. 2. DSC analysis of ternary chloride salts LiCl–KCl–$CaCl_2$ with different mass fractions under the Ar atmosphere.

Fig. 3. Specific heat capacity of the chloride salts.

Fig. 4. Vapor pressure of ternary chloride salts LiCl–KCl–$CaCl_2$ predicted using FactSage.

Fig. 5. Weight loss curves of salt 1 and salt 2 during the heating process under two kinds of different atmospheres. (a) Weight loss curves of salt 1 and salt 2 during the heating process under the argon atmosphere. (b) Weight loss curves of salt 1 and salt 2 during the heating process under the air atmosphere.

Fig. 6. The XRD of the ternary chloride salts with different components.

Fig. 7. TES heat capacity of the nitrate salts and chloride salts.

Fig. 8. DSC curves of the ternary chloride salts after 10 thermal cycles.

Fig. 9. XRD patterns of the ternary chloride salts before and after cycles.

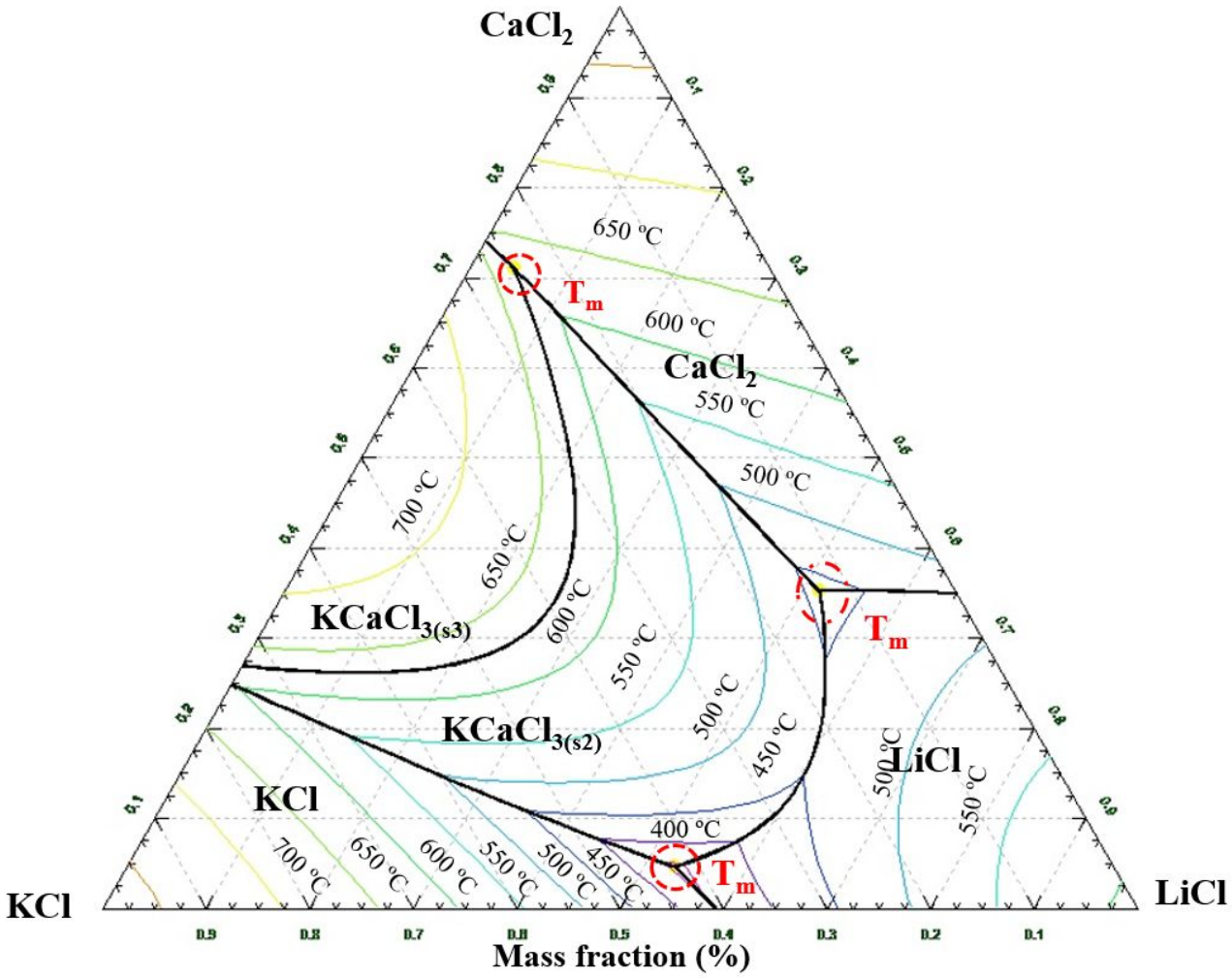

Fig. 1. Phase diagram modeled with FactSage, with the components predicted for ternary chloride salts LiCl–KCl–$CaCl_2$.